THERMODYNAMICS OF IMPACT GENERATED VAPOR PLUMES AFTER DISPERSAL OF THE SOLAR NEBULA. E. J. Davies[1], P. J. Carter[1], M. S. Duncan[2], S. T. Stewart[1], S. B. Jacobsen[3]. [1]U. California, Davis (ejdavies@ucdavis.edu), [2]Virgina Tech, [3]Harvard University.

Introduction: Impacts are a widespread and fundamental process during planet formation [1]. Recently, we demonstrated that a significant fraction of the mass of the inner solar system is subject to partially vaporizing collisions [2]. During the giant impact phase 10s of % of planetary mass can be processed as ejecta [3-5]. There can be even more partially vaporized debris when including planetesimal-planetesimal and planetesimal-embryo collisions [2]. It is important to understand the thermodynamic path of materials during impact events to be able to predict the chemical consequences. Vaporization during isobaric heating has different outcomes than vaporization during decompression after shock compression.

During isobaric heating, the material follows a thermodynamic path such as the dark blue arrow in Fig. 1. Free evaporation and removal of the vapor produces mass-dependent isotopic fractionation between the liquid and vapor. Shock-induced vaporization, however, follows a more complex thermodynamic path, such as A-C-D-E in Fig. 1. Material following this path within an impact vapor plume would not obtain the same isotopic fractionation as the free evaporation example.

Within the gas of the solar nebula, impact vapor plumes initially expand and then hydrodynamically collapse to form warm, dense 'clouds' [see 6, 7]. After the solar nebula disperses, a vapor plume that freely decompresses into empty space will follow an isentrope until the material becomes optically thin enough to radiatively cool.

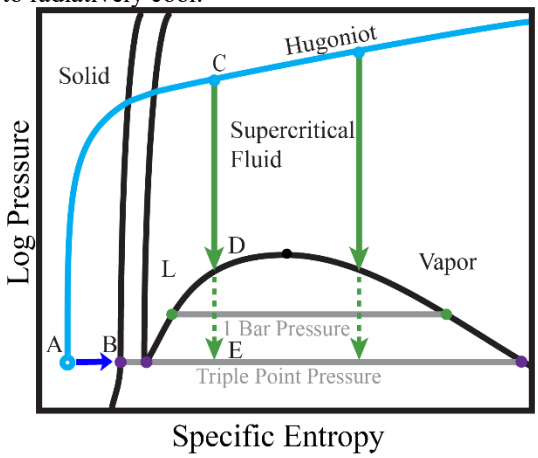

Fig 1: Schematic of a generalized single component phase diagram (black lines denote phase boundaries). The blue curve is the shock Hugoniot. Green lines show decompression along isentropes from specific shock states (blue points). In mixed phase regions, the mass fraction of each phase is given by the lever rule. The triple point pressure of silicates is similar to the fiducial pressure of the solar nebula at 1 AU, about 10^{-4} bar. Typical silicate critical point pressures range between 1 to 10 kbar. The dark blue line shows an example vaporization path at constant pressure.

Moderately volatile elements (MVEs), e.g., potassium, sodium, and rubidium, are defined as elements with 50% condensation temperatures between 650 K and 1300 K. Planets and meteorites have differing abundances of MVEs, with differentiated bodies typically more depleted relative to undifferentiated bodies [8]. The origin of this pattern is widely debated, and there are many proposed mechanisms: variations in the condensed fraction of dust in the solar nebula [e.g., 9], variable contributions from interstellar dust [e.g., 10], outgassing from magmatism [11], or impact events [12]. However, the processes that led to variations in MVEs cannot be accompanied by significant isotopic fractionation [8, 13]. Based on the thermodynamic path of vaporizing impact ejecta, we discuss how impacts may fractionate MVE abundances without significant fractionation of MVE isotopes.

Thermodynamic Path: Here, we consider impacts between rocky bodies during terrestrial planet formation, where vapor plumes are dominated by silicate compositions. We use the recently revised forsterite equation of state [14]. Shocked materials decompress via rarefaction waves, which are sound waves. Thus, in the absence of other processes, decompression is considered an isentropic process.

Upon reaching the intersection of liquid-vapor phase boundary, ejected materials with entropies above the critical point are vapor, while those below are liquid. Just below the intersection, decompression continues along the same isentrope, partially vaporizing the liquid (e.g., low specific entropy path in Fig. 1) or partially condensing liquid (high specific entropy path). The ejecta expands as a mixed phase system with liquid and vapor in equilibrium.

The vapor fractions of parcels of ejecta with different specific entropies are shown in Fig. 2. Starting at the intersection with the liquid-vapor dome, there is a massive volume increase even with a small vapor fraction. Note that a single parcel can experience both condensation and vaporization during isentropic decompression. When a silicate parcel has reached the pressures near the triple point (1–10 Pa), it has expanded into a plume 7 to 8 orders of magnitude larger than the volume of the un-shocked material. This volume is not the final volume of the plume, and in the absence of nebular gas the condensed plume continues to expand along ballistic trajectories.

The optical depth of the mixed phase liquid-vapor plume is controlled by the liquid droplets [15]. While

the optical mean free path is dependent on condensate size, in all cases, the mean free path only becomes large once the vapor plume is greatly expanded. Thus, only the surfaces of the expanding vapor plume can radiatively cool. Once optically thin, the bulk silicate vapor fraction condenses by radiatively cooling, and the liquid droplets will begin to freeze if they have not already begun to solidify by decompression below the triple points of the major phases.

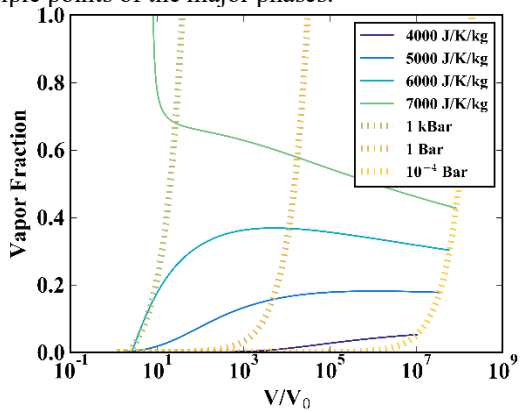

Fig 2: Vapor fraction versus the volume of decompressing forsterite normalized to the pre-shock volume using the new forsterite liquid-vapor dome [14]. Solid colored lines are isentropic release paths. Each path begins at the intersection of the liquid-vapor dome.

Liquid-Gas Interactions and Post Impact Dynamics: During decompression, the condensed and vapor components do not separate until the vapor pressures in the plume become negligible. The mixture of phases is inertially trapped in the expanding plume and do not separate during most of the expansion.

The relative proportions of liquid and vapor are established near the pressures where the isentrope enters the vapor dome. For example, the 6 kJ/K/kg isentrope in Fig. 2 reaches a vapor fraction of around 1/3 after expanding by a factor of 10 along the decompression path. At this point, the vapor pressures are near 1 kbar. During continued decompression, the proportion of vapor remains approximately constant. High vapor pressures diminish the effects of isotopic fractionation during partial vaporization or partial condensation in the vapor plume [8].

Figure 3 shows that while the temperatures and pressures are high, the mean free path of vapor atoms within the plume is very small, such that both the bulk silicate vapor and the liquid condensates are interacting under essentially equilibrium conditions. MVEs will strongly prefer the vapor phase at temperatures above the silicate triple point. When the system becomes optically thin, it rapidly quenches.

When the plume becomes optically thin and cools, the MVE-enriched vapor condenses as dust or condenses onto the surfaces of the freezing droplets. Surface area to volume ratios dictate that large droplets will have a lower mass fraction of recondensed vapor compared to small droplets. The smallest particles can be separated from the larger particles via mechanisms such as aerodynamic drag [16] (if some nebular gas remains), Poynting-Robertson drag, or radiation pressure [17].

If the ejected materials can be sorted by size prior to accretion into the final planetary bodies, then processing materials via vaporizing collisions can lead to changes in bulk MVE content without significant isotopic fractionation, as observed in planetary bodies [8].

Conclusions: (1) Shock-produced vapor is not strongly isotopically fractionated because of high vapor pressures followed by rapid freezing of the system. (2) After the vapor plume cools, different size particles should have different abundances of MVEs. Multiple mechanisms can separate different size particles. If ejecta is size sorted during accretion, MVE abundances can be perturbed by the cumulative effects of collisions.

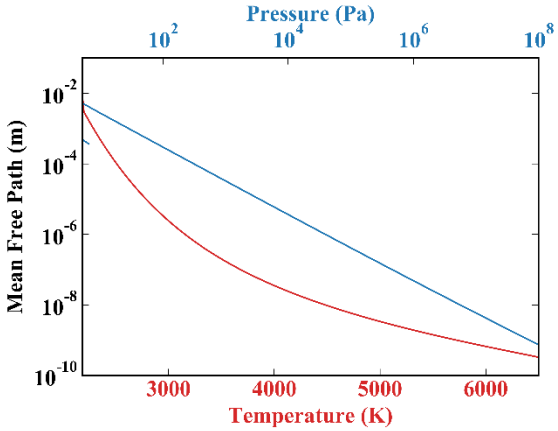

Fig 3: Mean free path of gas interactions (assuming silica atom cross section) during isentropic cooling (red) and decompression (blue).

Acknowledgments: This work is supported NASA grant NNX15AH54G; NASA grant NNX16AP35H (EJD); UC Office of the President grant LFR-17-449059; DOE-NNSA grants DE-NA0002937 and DE-NA0003904.

References: [1] Chambers, J. (2010) *Exoplanets* p. 297. [2] Davies, E. J., et al. (in revision) *JGR.* [3] Stewart S. T. & Leinhardt Z. M. (2012) *ApJ* **751**, 32. [4] Genda, H., et al. (2015) *ApJ* **810**, 136. [5] Genda, H., et al. (2017) *EPSL* 470: 87-95. [6] Stewart S. T. et al. (2019) *LPSC* ***50***, 1250. [7] Stewart S. T. et al. (2019) *LPSC* ***50***, 1251 [8] Davis A. M. (2006) MESS II, 295. [9] Cassen, P. (1996) *MPS* 31.6: 793-806. [10] Yin, Q. Z. (2005) *CPD* 341: 632. [11] Mittlefehldt, D. W. (1987) *GCA* 51.2: 267-278. [12] Halliday, A. N. & Porcelli, D. (2001) *EPSL* **192**, 545. [13] Humayun, M. & Clayton, R. N. (1995) *GCA* **59**, 2131. [14] Stewart. S. T., et al. (2019) *arXiv*: 1910.04687. [15] Kraus R. G. et al. (2012) *JGR: Planets* **117,** E9. [16] Adachi, I., et al. (1976) *PTP* **56**, 1756. [17] Burns, J. A., et al. (1979) *Icarus* **40**, 1.